ELSEVIER

Catalysis Today 83 (2003) 3–18

CATALYSIS TODAY

www.elsevier.com/locate/cattod

Status and perspectives of catalytic combustion for gas turbines

Pio Forzatti*

Dipartimento di Chimica, Materiali e Ingegneria Chimica "G. Natta" del Politecnico, Piazza Leonardo da Vinci, 32, 20133 Milan, Italy

Received 1 May 2002; accepted 18 March 2003

Abstract

This paper provides a review of the status and of the perspectives of catalytic combustion for gas turbines. First the development activities of catalytic combustion systems carried out in the last few years are reported. Then the relevant characteristics of PdO supported catalysts and of transition metal-substituted hexaaluminates (HAs), that have been most extensively considered for this application, are addressed. Next the use of mathematical modelling as a tool for the design and analysis of catalytic combustors is discussed. Finally a novel fuel-rich approach to catalytic combustion is illustrated and the perspectives for this technology are briefly outlined.

Keywords: Catalytic Combustion; Palladium supported catalysts; Hexaaluminates; Gas turbine

1. Introduction

The NO_x emission regulations in United States (US) are based on the National Ambient Air Quality Standards (NAAQS): the ozone standard is not attained in several areas (85% of the population in US), whereas the NO_x standard is usually attained but NO_x is deemed as ozone precursor. Attainment areas require the use of the Best Available Current Technology (BACT), which is now 9 ppm NO_x for natural gas-fired turbines. The non-attainment areas apply the Lowest Achievable Emission Rate (LAER) technology, irrespective of the economic implications. Today LAER is considered to be 2 ppm NO_x, with most permits considered at 3.5–5 ppm.

The technology currently practiced to control the NO_x emissions from industrial gas turbines involves either water/steam injection or lean premixed combustion. To meet the stringent emission regulations many installations include a selective catalytic reduction (SCR) unit to remove NO_x in the exhaust gases. Dry low NO_x (DLN) systems deliver NO_x emission levels of 15–20 ppm, the latest advanced version of these systems being designed for 9 ppm. Further significant reduction in NO_x emissions via the DLN approach may be precluded by flame stability problems.

Catalytic combustion has the potential to reduce the emissions of NO_x to near zero and to achieve ultra-low emissions of CO and unburned hydrocarbons (UHC) in natural gas-fired turbines. Besides catalytic combustion reduces the risk of blow-out or instability and dynamics during combustion, does not require the use of expensive cleanup systems and implies negligible efficiency loss compared to gas turbines with conventional flame combustion systems [1–4].

The costs of various NO_x control technologies have been compared in a recent report by Onsite Energy Corporation commissioned by DOE [5]. Gas turbines with small (5 MW), medium (25 MW) and large (150 MW) size have been considered and the following technologies have been analysed: water/steam

* Tel.: +39-02-23993238; fax: +39-02-70638173.
E-mail address: pio.forzatti@polimi.it (P. Forzatti).

0920-5861/$ – see front matter © 2003 Elsevier B.V. All rights reserved.
doi:10.1016/S0920-5861(03)00211-6

injection; DLN; conventional, low-T and high-T SCR; catalytic combustion; SCONOX. Although the cost values for the various technologies are constantly being reduced, the obvious advantage of primary measure, catalytic combustion, as opposed to secondary cleanup measures (SCONOX and SCR) in both reduction levels and cost are evident. The disparity in the cost impact between primary and secondary measures is particularly large for small gas turbines, that are deemed for the distributed generation market which in turn is threatened by strict environmental regulations.

The potential of catalytic combustion has been recognised since more than 30 years, but only recently this technology has been proven to be viable in commercial gas turbine service.

This paper provides a review of the status and of the perspectives of this technology. First the development activities of catalytic combustion systems carried out in the last few years are reported. Then the relevant characteristics of PdO supported catalysts and of transition metal-substituted hexaaluminates (HAs), that have been most extensively considered for this application, are addressed. Next the use of mathematical modelling as a tool for the design and analysis of catalytic combustors is discussed. Finally a novel fuel-rich approach to catalytic combustion is illustrated and the perspectives for this technology are briefly outlined.

2. Development of catalytic combustor systems

In a traditional flame combustion system compressed air and fuel are mixed, then combusted in a flame and the hot gases expand and drive the turbine. Cooling with bypassed compressed air of the hot gases is required to reduce the temperature for delivery to the turbine inlet in the range from 1200 to 1500 °C. In order to have a stable flame the fuel must be concentrated in the flame zone which results in a localised high temperature (around 1800 °C) with associated NO_x formation. In a catalytic flame-less combustor fuel and air are thoroughly mixed before entering the catalyst, the fuel–air mixture is ignited over the catalyst outside the flammability region, the combustion is completed at lower temperatures, and the combustor outlet temperature is in the range from 1100 to 1500 °C.

The most promising approach to catalytic combustion for gas turbines is based on the hybrid concept, and relies on upstream fuel–air premixing and two-stage combustion process: in the first stage a fraction of the fuel is oxidised over the catalyst and in the downstream second stage the fuel conversion is completed and the gases are heated to the desired combustor exit temperature. In order to handle the operation of a hybrid catalytic combustor when the inlet temperature is too low for catalyst light-off either a pre-burner or a downstream pilot fuel injector is used. The use of a downstream pilot fuel injector requires that at full load condition the inlet temperature to the catalyst bed is higher than the light-off temperature of the catalyst, and this is feasible in recuperate gas turbines and in turbines with high pressure ratio and high firing temperature.

Fig. 1 shows that the typical operating window for hybrid catalytic combustors is bounded by the following constraints: (i) the inlet gas temperature must be high enough to sustain the necessary catalytic activity; (ii) the adiabatic combustion temperature must be high enough to ensure complete burnout of HC and CO within the available residence time; (iii) the maximum temperature within the catalyst must be low enough to ensure long term catalyst durability. A good uniformity of inlet fuel-to-air ratio and of inlet gas temperature is mandatory to assure that conditions in all portions of the reactor are within the operating window. Fig. 1 also indicates an approximate operating window for a DLN combustion system and suggests that catalytic combustion offers advantages over DLN systems for operation at low adiabatic flame temperatures.

The catalytic combustion system that has been developed to the best so far is the XONON cool combustion system. Here all the fuel, except that required for the pre-burner, is fed to the catalyst but the extent of fuel oxidation that occurs within the catalyst structure is limited, and accordingly also the maximum catalyst wall temperature is limited. This is achieved by means of a proprietary catalyst design based on the temperature self-moderating characteristics of PdO/Pd system in methane combustion, the use of monolith metal supports with heat-exchange capabilities between nearby active and passive channels, and the use of a diffusion barrier. The peculiar features of PdO/Pd catalysts will be discussed later. Coupling of

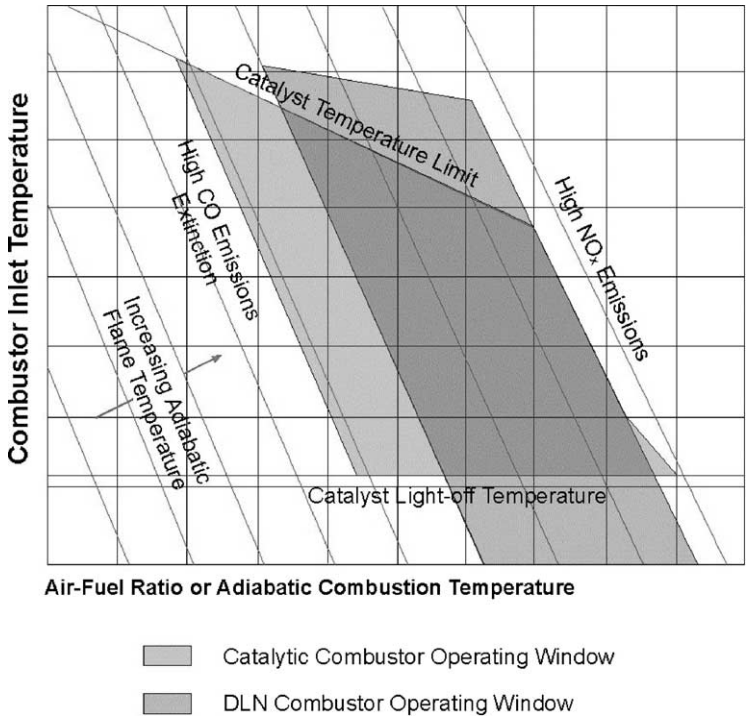

Fig. 1. Operating windows of catalytic combustion system and DLN system.

active and inactive channels is realised by arranging metal monoliths where the catalyst is applied to only one side of the monolith so that the heat generated inside the active channel is transferred to the nearby inactive channel by conduction through the wash-coat and the metal support. A diffusion barrier on the top of the active catalyst layer limits the supply of the reagents to the catalyst, and thus decreases the apparent activation energy of the combustion reaction. The catalyst section consists of an inlet stage designed to provide high catalytic activity, low light-off temperature and low catalyst wall temperature and one or more subsequent stages designed to operate at higher wall temperature in order to provide the required high outlet gas temperature. In a downstream section lean pre-mixed gas-phase combustion is accomplished, and CO and hydrocarbons are burned out to the levels required to meet the emission standards, and the combustor outlet temperature is raised to the levels of modern high efficiency gas turbines.

After extensive sub-scale, and full-scale, full pressure testing a 1.5 MW Kawasaki M1A-13A gas turbine was fitted with a XONON combustor, which utilises two catalyst stages and a lean premix pre-burner [6–8]. The test facility was connected with the electric utility grid at Silicon Valley Power in Santa Clara to validate the reliability, availability, maintainability and durability (RAMD) of the catalytic combustor system. The gas turbine package is controlled by a dedicated real time adaptive model control system. Average emissions of NO_x <2.5 ppm, CO <6 ppm, and UHC <3 ppm at full load have been maintained for more than 8000 h at the utility grid with very low dynamic pressure oscillations. The RAMD program, operating 24 h a day/7 days a week with commercial levels of unit availability (>90.5%) and excellent reliability (>98.5%), completed its program objectives on June 2001. The ultra-low emissions for this system have been verified by the Environmental Protection Agency.

Development activities of hybrid catalytic combustion systems have also been carried out in the last few years at General Electric for GE model MS9001E gas turbine, that has a turbine inlet temperature to the

first rotating stage of 1100 °C and produces approximately 105 MW in simple cycle operation [9], at Solar Turbines for the Mercury 50 machine that uses a recuperative cycle [10], at Siemens Westinghouse Power corporation for a lean premixed combustor that incorporates a catalytic pilot combustor and for a fully catalytic combustor [11], at Allison Engines for a proprietary machine developing 13.6 MW [12], at CRIEPI for a 20 MW class multi-can type gas turbine [13], and others. Most of these activities have been performed in the frame of the Advanced Turbine System program sponsored by the Department of Energy in US.

Based on the results of the development activities the following comments are in order:

1. Now it has been proved that catalytic combustion is a viable technology for natural gas-fired gas turbine commercial service. A service life of more than 8000 h has been demonstrated for 1.5 MW Kawasaki M1A-13A gas turbine, and operation at Silicon Valley Power will continue to demonstrate longer fired-hours service period and reliability.
2. The disparity in the cost impact between SCR and catalytic combustion is larger for small systems and this makes catalytic combustion particularly attractive for small gas turbine, that are considered for the distributed power generation market. The predictions for a significant growth in the world power plant market within the next 5–10 years indicate that there will be a large potential market for catalytic combustion in the near future.
3. There are indications that gas turbines with high firing temperatures (1400–1500 °C) may present the risk of catalyst overheating, considering that a substantial fraction of the fuel must be oxidised within the catalyst.
4. The integration of a catalytic combustor into a gas turbine requires dedicated development efforts. The operation of the catalytic combustion system fitted into the gas turbine is also a demanding task. Design, development and operation issues are certainly more demanding for multi-can than for single-can engines.

Therefore, one might expect that catalytic combustion will be applied at first to gas turbines with small or medium size, with single-can engine, and with not too high firing temperature.

3. Combustion catalysts

The combustion catalysts that have been most extensively investigated for gas turbine application are Pd-supported materials and metal-substituted HAs.

3.1. PdO-based catalysts

Palladium oxide supported on alumina or zirconia with various additives is the catalyst of choice for the combustion of natural gas in gas turbines in view of the following properties:

1. highest activity in methane oxidation, which results in low light-off temperature;
2. unique capability of temperature self-control due to the PdO–Pd metal reversible transformation. This transformation presents complex features that are not fully understood and that are likely responsible for the instability problems observed during pilot scale experiments;
3. low volatility of Pd species that may be present under reaction conditions.

The characteristics of the PdO–Pd transformation, its relevance to methane combustion, and the reaction kinetics are addressed below.

3.1.1. Characteristics of the PdO–Pd transformation

The decomposition and reformation of PdO during thermal cycling has been investigated in the literature primarily by means of TG and TPO analyses, and of in situ high-T techniques [14–18].

Reproducible TPO results obtained after the first heating–cooling cycle over PdO (10%) supported on γ-alumina stabilised with La_2O_3 and calcined at 1000 °C for 10 h are shown in Fig. 2. The decomposition of PdO during the heat-up cycle occurs in three distinct steps at different temperatures and the observed overall oxygen desorption corresponds well to the amount of PdO originally present. During the cool-down cycle the reformation of PdO from Pd is observed at temperature well below that of decomposition, thus originating a characteristic temperature hysteresis. PdO re-oxidation proceeds further in the subsequent heating ramp. Most of PdO is decomposed in the first two steps whereas the third one involves only a minor fraction of PdO, and both PdO and Pd

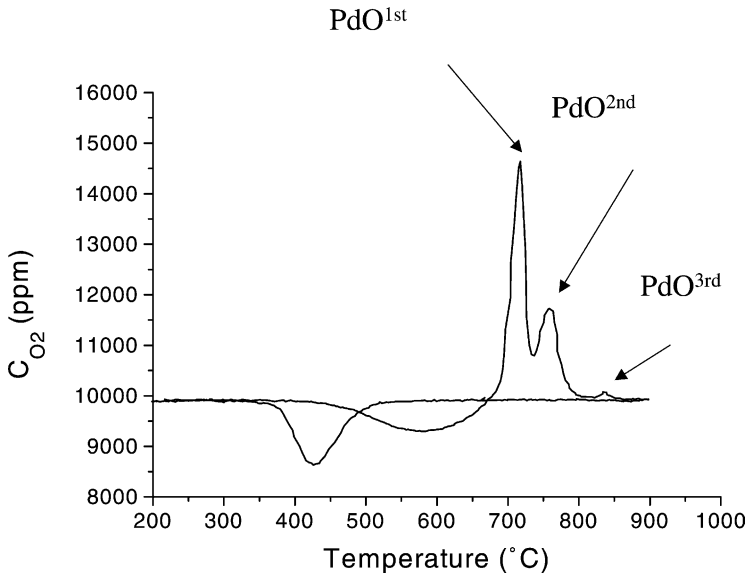

Fig. 2. TPO profiles of PdO decomposition (heating) and reformation (cooling) for PdO (10% w/w) supported on La_2O_3 (5% w/w) stabilised alumina calcined at 1000 °C for 10 h. Experimental conditions: heating/cooling rate = 20 °C/min in 1% O_2.

metal are present upon reformation. The three steps of PdO decomposition are associated with different oxide species, quoted in the following as PdO^{1st}, PdO^{2nd} and PdO^{3rd}.

TPO experiments over the same catalyst with holds during the heating ramp for different time periods and at different temperatures indicated that the oxidation of Pd metal occurs via the in series process Pd $\rightarrow$ PdO^{1st} $\rightarrow$ PdO^{2nd}, and that PdO^{2nd} is favoured at high temperature [17]. Notably PdO^{3rd} always represents a very small amount of the overall Pd (below 5%) for this catalyst. Besides for TPO experiments performed at different oxygen partial pressure a linear dependence was derived in terms of $\ln(P_{O_2})^{1/2}$ vs. $1/T_{D1}$, where T_{D1} is the temperature of onset of the first decomposition step of PdO, that compares well with data for bulk PdO and with thermodynamic data for the PdO/Pd system [19]. This indicates that the decomposition of PdO^{1st} is consistent with thermodynamics of the PdO/Pd system. A linear trend is also obtained for PdO^{2nd}, that is stable up to higher temperature, indicating that the decomposition of this species is consistent with thermodynamics of a different system, which however is believed to involve PdO as well.

Additional information on the PdO–Pd transformation over this catalyst has been provided by in situ high-T XRD with synchrotron radiation. The spectra confirmed the occurrence of the reversible PdO–Pd transformation in 2% O_2 atmosphere with the characteristic hysteresis described above. The Rietveld analysis of the spectra indicated that only one type of crystalline PdO is present, that corresponds to bulk PdO; the ratio of PdO to Pd metal compares well to the overall extent of re-oxidation ($PdO^{1st} + PdO^{2nd} + PdO^{3rd}$) as determined by TG and TPO measurements. Possible non-stoichiometry of PdO has been ruled out on the basis of the observed linear dependence of the thermal expansion of the unit cell with temperature [20]. Accordingly, the presence of important amounts of amorphous PdO_x, as originally proposed in the literature [17], can be excluded. The crystallite size, calculated by Rietveld refinement of the XRD spectra, is in the range 15–20 nm for PdO whereas that of Pd metal increases from 35 to 55 nm during heating and decreases from 55 to 35 nm during cooling with the characteristic temperature hysteresis of the PdO–Pd phase transformation.

The re-oxidation of Pd metal during the cooling ramp of the thermal cycle has recently been described

to occur via the formation of multiple incoherent PdO domains from the initial metal agglomerates on the basis of a detailed HRTEM and XPS study [21]. However, XRD data are also consistent with the growth of a PdO shell on the surface of the large metal particles followed by fragmentation due to lower density of the tetragonal PdO phase ($d = 8.15\,g/cm^3$) as compared to the fcc Pd metal phase ($d = 11.82\,g/cm^3$). In both cases the re-oxidation of Pd metal results at the beginning in the formation of PdO crystallites in boundary contact with metal Pd, that have been tentatively associated with PdO^{1st} [17]. Then PdO crystallites originating from the fragmentation process are formed, that are more isolated from the metal and are in physical contact with other PdO crystallites or with the support. These have been tentatively associated with PdO^{2nd} [17]. Finally, PdO^{3rd} has been associated with PdO strongly interacting with the support, in line with previous literature suggestions [22].

This picture is consistent with the peculiar features of the PdO–Pd reversible transformation observed over PdO (5% w/w) on La stabilised Al_2O_3 calcined at 500 °C for 10 h, where the formation of large Pd metal particles is prevented. In this case PdO^{1st} is present as a shoulder, PdO^{3rd} accounts for a large fraction of the overall amount of PdO, in particular after aging at high temperature under reaction conditions, and PdO reformation after cooling is almost complete so that further re-oxidation of the metal during the subsequent heating ramp is of minor importance. These data suggest that catalyst activation at low temperature (well below that of PdO decomposition) results in higher dispersion of palladium which in turn favours the re-oxidation of metal Pd and the strong interaction of PdO with the support after prolonged operation at high temperature.

While the data discussed so far refer to La stabilised alumina it is important to recognise that the nature of the support plays an important role in the PdO–Pd reversible transformation.

Table 1 summarises the TG results collected during thermal cycling in air over PdO supported on different alumina-based materials and calcined at different temperatures. It appears that (i) the temperatures of the first and the second steps of PdO decomposition are only marginally affected by the nature of the alumina support and by the calcination temperature; (ii) in the catalyst calcined at 500 °C PdO^{1st} is observed in minor amounts. Both points (i) and (ii) are in line with the mechanism of Pd metal re-oxidation previously discussed; (iii) PdO reformation during cooling is anticipated over CeO_2-promoted alumina materials and the re-oxidation of Pd metal during the subsequent heating ramp is of minor importance, due to the greater mobility of lattice oxygen.

Table 1
Temperature of onset of the first and second step of PdO decomposition during the heating ramp (T_{D1}, T_{D2}), and that of the re-formation of PdO from Pd during cooling (T_R) in thermal cycling in air at atmospheric pressure for PdO supported on different alumina-based materials and calcined at different temperatures

Support	Calcination, T (°C)	T_{D1} (°C)	T_{D2} (°C)	T_R (°C)
Al_2O_3	1000	795	835	690
La_2O_3–Al_2O_3	1000	800	840	690
CeO_2–Al_2O_3	1000	795	845	755
La_2O_3–CeO_2–Al_2O_3	1000	800	850	750
Al_2O_3	500	nd*	830	667
La_2O_3–Al_2O_3	500	790 (sh)**	830	661

* not detected.
** shoulder.

In the case of PdO (10% w/w) on ZrO_2-based supports (ZrO_2, SiO_2 (3.5% w/w)–ZrO_2, and La_2O_3 (7% w/w)–ZrO_2) the peaks corresponding to the first and second steps of PdO decomposition are poorly resolved and are observed at temperatures comparable to those of the alumina samples. Also the hysteresis is smaller and no significant re-oxidation is detected during the heating ramp, as in the case of CeO_2-promoted alumina samples [23]. Besides no evidence for the PdO^{3rd} species are observed.

The temperature hysteresis during thermal cycling has been tentatively associated with the capability of Pd metal to chemisorb oxygen only below the PdO reformation temperature T_R or to the formation of a passive layer of chemisorbed oxygen. The first explanation cannot account for the smaller extent of hysteresis observed for unsupported PdO as compared to supported PdO, and for its dependence on the nature of the support. The passive oxide layer on the surface of metallic Pd crystallites could suppress nucleation and growth of bulk PdO. Along these lines the nucleation and growth of PdO is favoured by the presence of oxidised Pd particles, even though not in boundary contact with the metal (PdO^{2nd}), as indeed observed in the case of partial decomposition of the oxide (decomposition

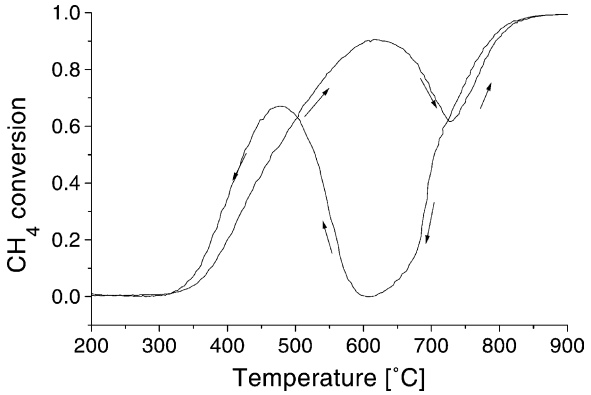

Fig. 3. TPC profile from the annular reactor. Experimental conditions: catalyst PdO (10% w/w) supported on lantania (5% w/w) stabilised alumina calcined at 1000 °C for 10 h; CH_4 = 0.5%, O_2 = 2%, H_2O = 1%, He = balance; GHSV = $10^6\,h^{-1}$; heating/cooling rate = 15 °C/min.

of PdO^{1st} only) [23] and of decomposition of unsupported PdO (where only a small fraction of bulk PdO undergoes decomposition) [17]. Likewise, the nucleation and growth of PdO is favoured over ZrO_2-based and CeO_2-promoted materials due to effective transfer of lattice oxygen.

3.1.2. Relevance of PdO–Pd transformation in methane combustion

Fig. 3 shows the conversion of methane obtained in a temperature programmed combustion (TPC) experiment performed using a structured annular reactor [16] at extremely high GHSV ($10^6\,h^{-1}$) and using PdO (10%) supported on lantania stabilised γ-alumina calcined at 1000 °C for 10 h. During heat-up methane activity is first noted at 340 °C, passes through a maximum at 620 °C (with 90% conversion) and then through a minimum at 730 °C, and eventually rises again to almost complete conversion at 860 °C. When the temperature is reversed and only Pd metal is present the activity is very poor and passes through a marked minimum at 620 °C, and then suddenly increases showing a maximum of 70% conversion near 460 °C and effectively overlapping the curve generated during heat-up.

The data in Fig. 3 confirm that PdO is much more active than metallic Pd. Also a nice correspondence is observed between the hysteresis observed during thermal cycling for the PdO–Pd transformation and the hysteresis in the conversion of methane shown in Fig. 3. Indeed comparison with TPO profiles with relevant O_2 concentration (1 and 2% O_2) has shown that during the cooling ramp the restoration of combustion activity begins at the temperature of onset of PdO reformation and is complete at 460 °C when only a small fraction of the oxide species PdO^{1st} has been formed. This is in line with previous literature results [22,24] obtained during low temperature oxidation of metallic Pd which indicate that activity increases until very few monolayers [4–7] of PdO are formed, where-after the activity does not increase with further oxidation. Likewise during heat-up the conversion begins to decrease approximately at the onset of the PdO decomposition, but deviation from the Arrhenius trend is observed well below this temperature. Here the influence of diffusion limitations has been ruled out on the basis of theoretical calculations [25]. It is worth noting that the data collected at high temperature tanks to the peculiar features of the annular reactor provide indications on the catalytic behaviour under chemical regime in a temperature range that could not be investigated previously.

To further study the effect of the dynamics of PdO decomposition–re-oxidation on methane combustion activity TPC experiments with temperature holds for several minutes during the cooling and heating ramps have been performed in the annular reactor. It has been observed that: (i) during cooling no activity gain occurs with time at temperature above that of the onset of Pd metal re-oxidation to PdO whereas activity increases sharply with time and to a great extent immediately below that temperature. This confirms that PdO^{1st} is much more active than Pd metal; (ii) activity decreases slightly with time already at 450 and 550 °C, and more markedly at 550 °C during heat-up. Considering that in this temperature range, that is well below that of PdO decomposition, PdO^{1st} is transformed into PdO^{2nd} the data suggest that the former species is more active than the second one. Besides TPC experiments were also performed in the annular reactor over the catalyst that was pre-treated in order to contain primarily the species PdO^{1st} + Pd metal (upon re-oxidation of the catalyst during the cooling ramp) or PdO^{2nd} (upon re-oxidation during cooling followed by re-oxidation during heating up to 600 °C). The TPC curves are shown in Fig. 4. The heating branches of the TPC runs clearly demonstrate the lower reactivity of species PdO^{2nd} as compared to species PdO^{1st}, whereas the

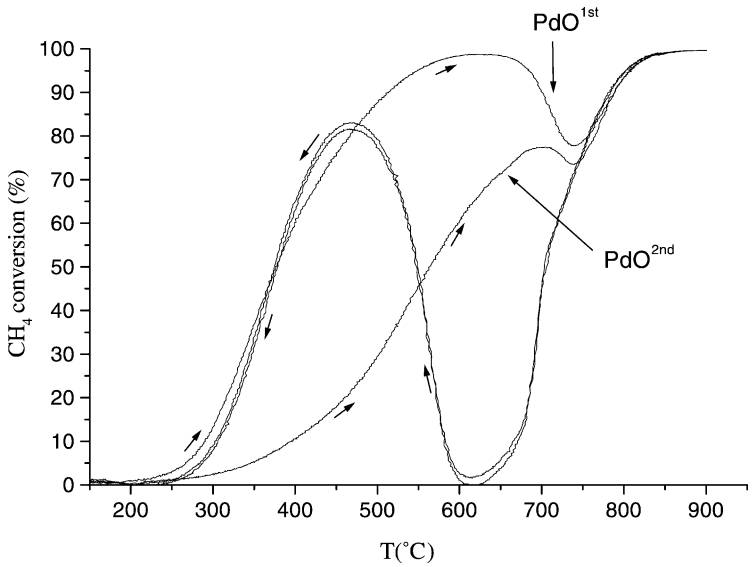

Fig. 4. TPC of methane in the annular reactors over PdO (10% w/w) supported on lantania (5% w/w) stabilised alumina at 1000 °C for 10 h after the following pre-treatments: cooling in 1% O_2 at 15 °C/min (PdO (primarily PdO^{1st}) + Pd metal); cooling in 1% O_2 at 15 °C/min + heating in 100% O_2 at 15 °C/min up to 600 °C + 2 h at 600 °C in 100% O_2 + cooling in 100% O_2 at 15 °C/min (PdO (primarily PdO^{2nd}) + Pd metal). Experimental conditions: catalyst; $CH_4 = 0.5\%$, $O_2 = 2\%$, $H_2O = 1\%$, He = balance; GHSV = $10^6\ h^{-1}$; heating/cooling rate = 15 °C/min.

cooling branches are almost superimposed as expected since in both cases re-oxidation proceeds in a similar way from Pd metal. The higher reactivity of species PdO^{1st}, that has been identified as PdO in boundary contact with metallic Pd, is likely associated with such intimate contact that has already been invoked in the literature to account for the increase in catalytic activity upon partial reduction of PdO. This may be ascribed either to a direct role of metallic Pd sites in the activation of methane through dissociative adsorption [26,27] or to the presence of high defectivity in the vicinity of Pd/PdO boundary. Besides a contribution of PdO crystal size to the different reactivity observed in Fig. 4 for the two PdO species cannot be ruled out.

3.1.3. Kinetics of methane combustion over PdO catalysts

The measurement of the activity of PdO catalyst in methane combustion and the assessment of reliable reaction kinetics under representative conditions is an issue of both fundamental and practical importance.

Usually the activity in methane combustion is reported in the literature in terms of turnover rates (TOR) based on the number of Pd atoms counted on the reduced catalyst by means of surface titration or chemisorption, and is confronted with the size of Pd metal crystallites. These values are widely scattered, as shown in Table 2. It has been noted that these initial dispersion measurements for metallic Pd may not represent the actual dispersion present under reaction conditions, because both oxidation state and morphology of the particles are modified under reaction

Table 2
Comparison of TOR for the oxidation of methane over supported catalysts (after [28])

TOR[a]	Particle size (nm)	E (kJ/mol^{-1})	Reference
7×10^{-3} to 1×10^{-1}	1.4–5.6	71–84	[29]
1×10^{-4} to 2×10^{-3}	1–30	110–125	[30]
3×10^{-3}	3	–	[31]
3×10^{-2}	16	–	[32]
1×10^{-4} to 2×10^{-2}	2–80	80–160	[33]
2×10^{-2} to 8×10^{-1}	2–110	75–90	[28]

[a] Rates calculated for a reaction temperature of 559 K in 2% CH_4/air using the activation energy and the reaction orders given in the original publications. When the reaction order data were not available, the reaction orders were assumed to be 0 and 1 for O_2 and CH_4, respectively.

conditions. Besides incomplete activation of the samples, the widespread neglect of product inhibition which, obviously, would vary with the conversion, and the features of the PdO–Pd transformation that are relevant for methane combustion activity may have contributed to the lack of agreement among the reported TOR. After taking into accounts all these factors, Ribeiro et al. [28] concluded that TOR values are only marginally affected by the Pd crystallite size. However, other authors arrived to the opposite conclusions [34,35] and published a clear correlation between TOR and particle size of Pd metal [35]. Accordingly this point is still under debate.

In this respect it is also important to note that PdO and not Pd is recognised by several authors as the active phase in methane combustion, and that the surface area of the oxide is higher than that of the metal after re-oxidation [36,37]. In view of this Ribeiro and co-workers [38,39] recently proposed to measure the PdO surface area by means of exchange experiments using labelled oxygen. The exchange experiments consisted of exposing the oxidised Pd catalyst to $^{18}O_2$ conditions selected on the basis of the work of Au-Yeung et al. [40] and designed to ensure that the exchange may happen only at the surface with no appreciable diffusion in the bulk. The amount of ^{18}O exchanged was measured in a TPD experiment by quantifying all the desorbed compounds containing ^{18}O. Ribeiro and co-workers compared reaction rates obtained over the Pd metal foil employed in the study after different activation treatments (i.e. none, excess methane and excess methane followed by reaction in excess oxygen) with the amount of oxygen exchanged and concluded that the rate of methane conversion is directly proportional to the PdO surface area. This approach is certainly of interest. However, it is still questionable whether it can be applied to supported PdO catalysts, since it has been observed that PdO facilitates the exchange of O with the support (in the case of ZrO_2), the exchange increasing with decreasing size of the PdO particles [40].

The methane combustion was found to be first order with respect to methane and zero order with respect to oxygen. Ribeiro et al. [28] reported that the reaction rate is not affected by CO_2 up to 0.5% by volume, whereas above this amount the reaction order is -2. However, inhibition by CO_2 was not confirmed by other authors [41]. Water has a pronounced affect on the rate [28,41]. An apparent activation energy of 70–90 and $\approx$150 kJ mol^{-1} have been measured under dry and wet conditions, respectively [28,29,41,42]. Such values of the apparent activation energy can be reconciled if water inhibition is properly accounted for in the analysis [41]. Fujimoto et al. [35] proposed the reaction pathways shown in Table 3 where the rate determining step is represented by the dissociative chemisorption of CH_4 on a site pair consisting of adjacent Pd surface vacancies and surface PdO species. The scheme explains the inhibition by CO_2 and H_2O because these products titrate vacancies on PdO surfaces via the reverse of desorption steps 5–7 in Table 3. Notice that the mechanism avoids the need for the coexistence of a separate Pd metal phase in contact with PdO during methane oxidation.

Table 3
Proposed reaction pathways for the oxidation of methane on PdO_x crystallites[a]

$O_2 + {}^* \leftrightarrow^{K_1} O_2{}^*$	(1)
$O_2 + {}^* \overset{k_2}{\rightarrow} 2O^*$	(2)
$CH_4 + {}^* \overset{K_3}{\leftrightarrow} CH_4{}^*$	(3)
$CH_4{}^* + O^* \overset{k_4}{\rightarrow} CH_3{}^* + OH^*$	(4)
$2OH^* \overset{K_5}{\leftrightarrow} H_2O(g) + O^* + {}^*$	(5)
$CO_2{}^* \overset{K_6}{\leftrightarrow} CO_2 + {}^*$	(6)
$CO_3{}^* \overset{K_7}{\leftrightarrow} CO_2 + {}^*$	(7)

[a] Asterisk denotes coordinatively unsaturated surface Pd atoms.

However, kinetic studies in the literature have been customarily performed under conditions far from those of real interest, namely at low GHSV, low temperature, atmospheric pressure, and using a microflow reactor operated with diluted gas feed at low conversions. Therefore, extrapolation of the kinetics to actual operating conditions is critical and must be properly checked. This has been attempted for instance by studying the effect of combustion products on the ignition performance of the catalyst by Dalla Betta et al. [43]. The reaction was accomplished in a 50 mm diameter catalyst at 11 atm and with a flow rate of 9300 SLPM. The feed gas was heated and cooled at 5 °C/min while the methane/air ratio was varied to maintain the adiabatic temperature of 1300 °C. A temperature shift of 18 °C for ignition was observed

when replacing electrical preheating with the pre-burner in order to provide in both cases a 200 °C temperature rise. Considering that 200 °C temperature rise from the pre-burner results in CO_2 and H_2O concentrations in the range where strong inhibition has been reported by the same research group [28] it was concluded that inhibition is strongly temperature dependent, and at 350–400 °C the inhibition may be significantly reduced.

Therefore, in order to develop representative kinetics it is mandatory to collect kinetic data under conditions as close as possible to the real ones. In this respect both the annular reactor proposed by McCarty [16] and the reactor cell employed by Lyubovsky and Pfefferle [27], that are schematically shown in Fig. 5, represent promising kinetic devises. The annular reactor consists of a ceramic tube coated with a thin catalyst layer and co-axially placed inside a quartz tube to form an annular chamber where the gas flows straightforward. In the other reactor the sample plate, after deposition of the catalyst in the form of a thin layer, is placed into the reactor holder to form a thin space over the catalyst surface where the gas flows. Both reactors allow operation at extremely high GHSV and with negligible pressure drop so that kinetic data with partial methane conversion can be collected at high temperature. An engineering analysis of the annular reactor has been developed [25], which demonstrated that inter-phase and intra-phase heat and mass transfer limitations do not significantly affect the reactor performance in the case of methane combustion for appropriate value of the thickness of the catalyst layer and of the height of the annular section, and besides that the removal of the heat of reaction is very effective and it occurs primarily by radiation already at 500 °C.

By using the annular reactor kinetic investigations which cover a higher temperature region than in the past have been attempted over PdO supported on alumina and zirconia [25,44]. In the case of PdO on alumina the data are affected by deactivation phenomena. However, the data clearly showed that H_2O strongly inhibits the reaction up to 600 °C, while no inhibition was measured for CO_2 at 500 °C. On the contrary, PdO on zirconia was found to be fairly stable up to 550 °C. In this case methane combustion is inhibited by both water and carbon dioxide, the inhibiting effect of water over PdO on zirconia being smaller than over PdO on alumina. These data provide evidence for an important effect of the support on the performance of PdO catalysts.

3.2. Transition metal-substituted HA catalysts

HA materials containing transition metal ions in the structure have been extensively investigated for gas

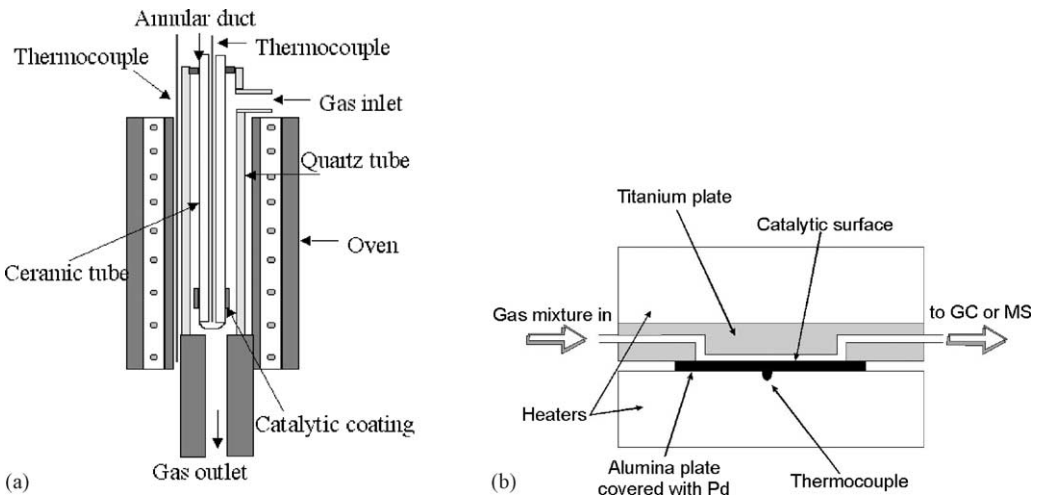

Fig. 5. Schematic diagram of the annular reactor proposed by McCarty [16] and of the reactor cell employed by Lyubovsky and Pfefferle [27].

turbine applications, in view of their excellent thermal stability and catalytic activity.

These materials can be prepared by hydrolysis of the alkoxides [45] or by co-precipitation from soluble salts of the constituents by using NH_4OH or $(NH_4)_2CO_3$ as the precipitating agent [46]. Monophasic samples with surface area in the range 10–15 m^2/g are obtained upon calcinations at 1300 °C. The high-T thermal stability of these materials is associated with their peculiar layered structure that consists of closely packed γ-Al_2O_3 spinel blocks separated by mirror planes that contain large alkali, alkali-earth and rare-earth ions (Ba, Ca, La, and Sr) and loosely packed oxygen ions. Two structures are possible (Fig. 6): β-Al_2O_3 and magnetoplumbite (MP), that differ in the composition of the mirror plane. Spinel blocks and mirror planes are alternatively stacked, originating an hexagonal structure with the *c*-axis parallel to the direction of stacking. These materials crystallise as hexagonal planar particles with strong anisotropic shape, because the grain growth along the direction of the *c*-axis is suppressed due to inhibition of ions diffusion along the stacking direction [47].

In view of the close similarity of ionic radii, transition metal cations can partially substitute Al ions, thus providing significant methane combustion activity to the catalyst. Mn-substituted HA catalysts are most active. Mn enters the structure at low concentration preferentially in tetrahedral Al sites with dominant oxidation state +2, with reduction of Ba vacancies in the mirror plane according to a charge compensation mechanism, and at high concentrations in octahedral Al sites with dominant oxidation state +3 [48]. The catalytic activity is also influenced by the composition of the mirror plane: maximum methane combustion activity has been reported by Arai and co-workers for $Sr_{0.8}La_{0.2}Mn_1Al_{11}O_{19}$ [49]. This activity is comparable, however, to that of $BaMn_2Al_{10}O_{19}$ [50] and it is even slightly lower than that recently measured over $LaMg_{0.5}Mn_{0.5}Al_{11}O_{19}$ [51]. It has been suggested that the incorporation of a divalent cation such as Mg^{2+} stabilises the MP structure via a charge compensation mechanism that lowers the defectivity of the material and prevents segregation of $LaAlO_3$, that may result in additional sintering of the final material. Besides the presence of Mg^{2+} favours the incorporation

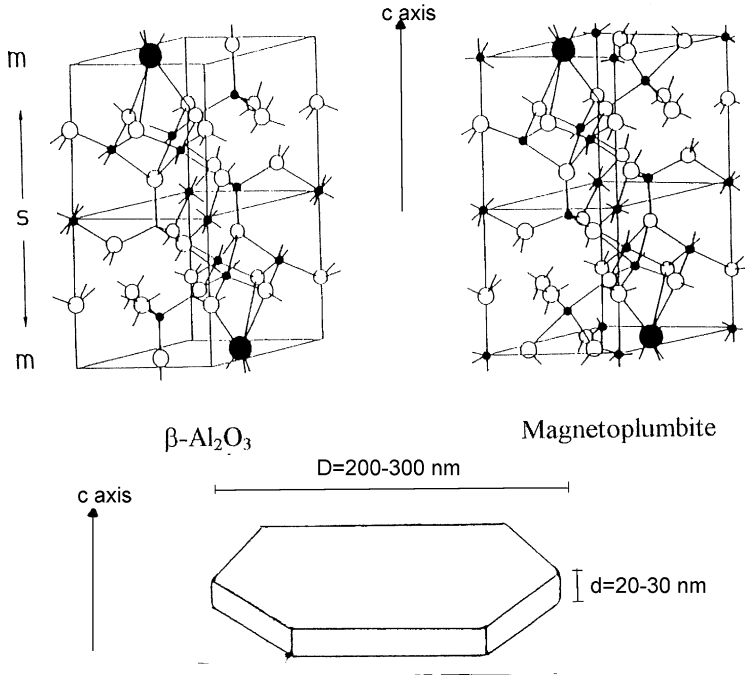

Fig. 6. Ideal semicell of β-Al_2O_3 and MP structures: (•) large cations, (○) oxygen anions, and (●) aluminium ions and sketch of the thin planar crystallites of HAs.

of Mn as Mn^{3+}, which likely explains the higher catalytic activity of this system.

Recently, through a reverse-micro-emulsion mediated synthesis Ba-hexaaluminate (BHA) nanoparticles were crystallised directly to the desired phase at a relatively low temperature of 1050 °C, and sustained surface areas in excess of 100 m^2/g after calcination at 1300 °C for 2 h [52,53]. In this technique nanometer-sized aqueous micelles dispersed in the oil phase represent nano-reactors for controlled hydrolysis and condensation of Ba and Al alkoxides. Since the diffusion of the precursors through the oil phase is the rate limiting process and Ba and Al alkoxides have similar diffusivity in the oil, they were homogeneously reacted within the aqueous nano-domains of the reverse micro-emulsion. To tailor the particle morphology, structure and surface area of the BHA nanoparticles synthesis parameters, and drying conditions had to be carefully controlled. This technique appears promising for the synthesis of bulk HA materials that can be employed as high-T thermally stable supports for catalytic combustion.

4. Modelling of catalytic combustors

Mathematical models represent a powerful tool for the design and analysis of catalytic combustors for gas turbines. Single channel models have been customarily used to describe catalytic combustors, which appears reasonable considering that global adiabatic conditions and uniform distribution of the variables at the catalyst inlet section are approached in reality.

In principle many physical and chemical phenomena that occur within the reactor need to be considered, including: (i) heterogeneous reactions in the catalyst and homogeneous reactions in the gas phase; (ii) heat, mass and momentum transfer by convection and diffusion in the gas phase and at the gas–solid inter-phase, that are affected by entrance effects; (iii) mass diffusion in the active catalyst layer; (iv) radial and axial heat transfer in the solid phase through the active washcoat and the ceramic or metallic substrate by conduction and radiation.

Models differ in physical and chemical complexity. The most comprehensive physical models are based on the solution of the Navier–Stokes equations, considering both axial and radial dispersion, momentum, and energy transport. These models are computationally expensive, difficult to develop and often difficult to use. An alternative is represented by models based on the boundary layer equations that retain a detailed mass and heat transport description to and from the channel wall, wherein the axial diffusive transport is neglected in view of the high gas velocity. The momentum balance can also be included in these models. The models based on the boundary layer equations represent a significant reduction in computational expense compared to Navier–Stokes formulation. Plug-flow 1D models, that are based on the lumping of the variables over the cross-section into appropriate average values, have also been used for preliminary design purposes in spite of the fact that they provide only an approximate description of the light-off performances and of heterogeneous–homogeneous interactions. These models are relatively simple to write and easily solved, but they require reliable correlations for mass and heat transfer coefficients. These correlations are not well established in particular for transitional and turbulent flow conditions that prevail under most operating regimes of catalytic combustors for gas turbine under pressure. For what concerns the description of the chemical processes it is worth noting that the catalytic and gas-phase contributions to fuel conversion are de-coupled in the hybrid configuration of catalytic combustors. A detailed mechanism that could capture the relevant and complex features of PdO catalyst is not available yet, although it is presently under development [54,55]. Accordingly, the surface chemistry is usually described by simple kinetics that can also incorporate catalyst aging. On the other hand, gas-phase chemistry is usually described by using detailed and well established mechanism such as that used in CHEMKIN [56].

Mathematical models have been employed in the literature for several purposes including: (i) design of the catalytic and homogeneous section for different combustor configurations (e.g. conversion performances, emissions, pressure drops, *T* profiles, thermal stresses); (ii) analysis of the combustor performances (e.g. conversion performances, emissions, pressure drops, *T* profiles, thermal stresses); (iii) extrapolation of laboratory data (e.g. light-off predictions, conversion performances); (iv) fundamental studies providing insight on the role of the different physicochemical phenomena occurring inside the combustor. Examples

for the use of mathematical modelling for design and analysis purposes can be found in [54,57–63].

5. Novel fuel-rich approach to catalytic combustion

The conventional approach to catalytic combustion involves the complete oxidation of lean methane/air mixture to CO_2 and H_2O with parallel release of heat. A fuel-rich approach to catalytic combustion for gas turbines has been recently proposed [64]. In this approach fuel is mixed with air to form a fuel-rich mixture that is reacted over the catalyst to produce both partial and total oxidation products. The reaction products are then mixed with excess air and burned to completion downstream in a homogeneous flame. Well mixed H_2 stabilised lean combustion can be realised in the post-catalyst zone and the maximum catalyst wall temperature can be controlled through appropriate tuning of the air–fuel ratio.

Catalytic partial oxidation of methane and light paraffins is envisaged and currently studied as a novel route to H_2 production. Mixed oxides (Ni, Co, Fe) and noble metals (Pd, Rh, Ru, Pt, Ir) have been reported to be active in the partial oxidation of methane to synthesis gas [65]. The observed performances (degree of methane conversion and the yields of CO and H_2) vary with the catalysts and the operating conditions but all reported data share these common features: (1) the product mixtures consists in CO, H_2 and CO_2 and H_2O, (2) all reported conversions and selectivity to CO and H_2 are below or approach the values corresponding to the thermodynamic equilibrium.

The direct reaction of methane partial oxidation always competes with total oxidation reactions, that are responsible for O_2 consumption as well, whereas steam and dry reforming and C-forming reactions are also to be considered. All reactions are catalysed by the materials which are active in partial oxidation, but different scales of reactivity for the catalysts can be estimated from the experimental data.

Total oxidation prevails at the light-off of the fuel-rich stream over most of the catalysts, but precious metals are more active than transition metals. It should be considered that the concept of light-off in a fuel-rich stream is different from the traditional definition in combustion. In partial oxidation, light-off is accompanied by the sudden consumption of the limiting reactant (oxygen); oxygen conversion instantly rises to 100% in packed bed reactors, or to finite values in structured reactors with inter-phase mass transfer limitations. Burch and Loader [66] have well explained that over Pt catalysts the methane combustion reaction is first order in methane but either zero order or, at low oxygen partial pressures, negative order in oxygen. Therefore, in some cases oxygen is seen to poison the catalyst. This has been interpreted in terms of there being a competition for adsorption sites between methane and oxygen. As a result, light-off temperature can decrease with increasing HC/O_2 ratio. This has been reported by several authors [65]. We also have observed a shift towards lower temperatures of the light-off in fuel-rich oxidation, when studying the partial oxidation of ethane over a Pt/Al_2O_3 catalyst, as shown in Fig. 7.

For steam and dry reforming the following scale of reactivity exists over precious and transition metals [68,69]:

$$\text{Ru, Rh} > \text{Ni} > \text{Pd, Pt} \gg \text{Co, Fe}$$

It has been noticed that there is a substantial similarity between the orders of activity of the metals for partial oxidation of methane and the orders of activity of the same metals for steam and dry reforming of methane [70].

Given the relative reactivity of the catalysts, selection of the catalyst and of the operating conditions can result in the different prevailing of a mechanism for CO and H_2 formation.

Rh is extremely active both in the direct and secondary reactions and this explains why rhodium is the catalyst of choice for the ultra-short contact time applications which have been extensively studied by Schmidt and co-workers [71–73]. It must be noted that the short contact time reactors are typically operated under adiabatic conditions with outlet temperatures in the order of 700–1000 °C. Besides, with respect to other noble metals, Rh is believed especially stable due to a low vapour pressure and an increased resistance to carbon formation even under severe operating conditions.

Direct and indirect reactions are likely involved in H_2 production under extreme operating conditions. Basini et al. [74] have published the results of methane partial oxidation runs in a pilot scale reactor

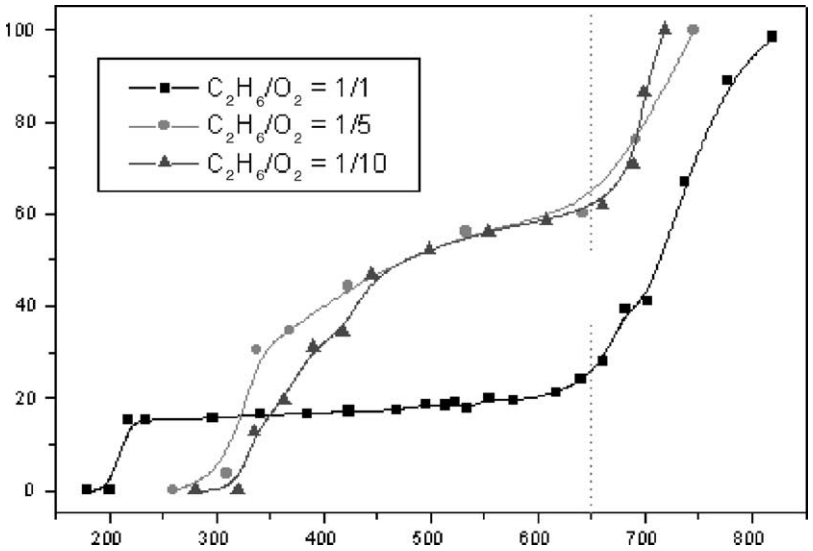

Fig. 7. Effect of C_2H_6/O_2 ratio on light-off. Experimental conditions: catalyst, 0.5% Rh–Al_2O_3; flow rate = 1 N l/min; weight of catalyst = 50 mg; feed composition, $C_2/O_2/N_2 = 3/x/97 - x$ [67].

operating at high pressure and short contact time, showing stable activity (almost complete conversion of methane and over 90% selectivity to CO and H_2) along over 500 h on stream. Under ultra-short contact times Pt appears less selective to H_2 than Rh, and this can be explained by a lower intrinsic activity towards direct partial oxidation and secondary steam and dry reforming reactions. However, syngas production over Pt–Pd monoliths have been demonstrated at the pilot scale when operating at lower space velocities (max. 300,000 h^{-1}); under these conditions, axial temperature and concentration profiles have evidenced that an indirect reaction mechanism with initial oxygen consumption through oxidation reactions followed by endothermic secondary reactions explained the production of CO and H_2 [75]. In the case of indirect mechanism, the application of a Ni catalyst or a combination of Pt and Ni catalysts (the first in charge of deep oxidation, the latter in charge of H_2 production through steam and dry reforming) has also been studied in the literature [65].

A number of additional advantages have been claimed for the fuel-rich approach to catalytic combustion for gas turbines as compared to the lean fuel approach. In addition to the stabilising effect of H_2 on downstream lean combustion and better control of the catalyst temperature, the fuel-rich approach allows for lower catalyst light-off so that the use of the pre-burner may not be necessary, flashback into the catalytic reactor is not possible, and fuel nitrogen may be converted to N_2 under rich conditions. These potential advantages must be proven at the sub-scale and full-scale, full pressure levels.

6. Conclusions

It has now been demonstrated that catalytic combustion is a viable technology for natural gas-fired gas turbine commercial service: a service life of more than 10,000 h has been demonstrated for 1.5 MW Kawasaki M1A-13A gas turbine [63]. For both economic and technical reasons catalytic combustion appears today particularly attractive for small size gas turbine with single-can engine and not too high firing temperature. Catalytic combustion has demonstrated several advantages over DLN, including lower NO_x emissions, stable combustion under very lean conditions (less noise) with ultra-low emission of CO and UHC, no flame out and more uniform T at the combustor outlet. It is expected that these benefits together with extension of the catalyst life (e.g. from 8000 to 16,000 h) and additional cost reduction could soon result in the commercialisation of catalytic combustion systems.

Supported palladium oxide is recognised as the catalyst of choice for the combustion of natural gas in gas turbines. Several fundamental issues related to this catalyst system are still open and their better understanding will certainly result in further improvement of the technology and will also benefit the abatement of methane emissions from compressed natural gas vehicles, which requires the use of PdO catalysts as well. These issues include the assessment of the active sites for methane combustion and their dynamics with respect to the PdO–Pd reversible transformation, the low temperature activity of PdO catalysts and methods to measure the surface area of PdO, and the reaction kinetics under conditions representative of full scale, full pressure gas turbine operation. Fundamental research is also recommended in the area of mathematical modelling.

Besides further development of high-T thermally stable and active catalysts (HAs, and possibly other materials) may be required along with a more extensive investigation of hydrodynamic (and chemical) methods for stabilising gas-phase combustion in the post-catalyst zone in order to apply catalytic combustion to gas turbines with firing temperatures in the range 1400–1500 °C.

Finally, the novel fuel-rich approach to catalytic combustion for gas turbines might represent a challenging alternative to the conventional lean-fuel approach in view of the additional advantages that have been claimed. The potentiality of this approach, however, need to be confirmed through more extensive testing at the sub-scale and full scale, full pressure levels.

Acknowledgements

This work was supported by MIUR, Rome (Italy).

References

[1] L.D. Pfefferle, W.C. Pfefferle, Catal. Rev. Sci. Eng. 29 (1987) 219.
[2] R.E. Hayes, S.T. Kolaczkowski, Introduction to Catalytic Combustion, Gordon and Breach, Amsterdam, 1997.
[3] R.A. Dalla Betta, Catal. Today 35 (1997) 129.
[4] P. Forzatti, G. Groppi, Catal. Today 54 (1999) 165.
[5] Onsite Energy Corporation, Cost analysis of NO_x control alternatives for stationary gas turbines, November 5, 1999.
[6] R.A. Dalla Betta, T. Rostrup-Nielsen, Catal. Today 47 (1999) 369.
[7] R.A. Dalla Betta, S.G. Nickolas, C.K. Weakley, K. Lundberg, T.J. Caron, J. Chamberlain, K. Greeb, ASME Paper 99-GT-295, 1999.
[8] D.K. Yee, K. Lundberg, C.K. Weakley, ASME Paper 2000-GT-0088, 2000.
[9] K.W. Beebe, K.D. Cairns, V.K. Pareek, S.G. Nickolas, J.C. Schlatter, T. Tsuchiya, Catal. Today 59 (2000) 95.
[10] P. Dutta, D.K. Yee, R.A. Dalla Betta, ASME Paper 97-GT-497, 1997.
[11] D.B. Fant, G.S. Jackson, H. Karim, D.M. Newburry, P. Dutta, K.O. Smith, R.W. Dibble, J. Eng. Gas Turbines Power 122 (2000) 293.
[12] D.A. Smith, S.F. Frey, D.M. Stansel, M.K. Razdan, ASME Paper 97-GT-311, 1997.
[13] Y. Ozawa, Y. Tochihara, N. Mori, I. Yuri, J. Sato, K. Kagawa, 5IWCC, Seoul, 2002.
[14] R.J. Farrauto, M.C. Hobson, T. Kennelly, E.M. Waterman, Appl. Catal. A 81 (1992) 227.
[15] R.J. Farrauto, J.K. Lampert, M.C. Hobson, E.M. Waterman, Appl. Catal. B 6 (1995) 263.
[16] J.G. McCarty, Catal. Today 26 (1995) 283.
[17] G. Groppi, G. Artioli, C. Cristiani, L. Lietti, P. Forzatti, Stud. Surf. Sci. Catal. 136 (2001) 345.
[18] S.J. Cho, S.K. Kang, J. Phys. Chem. 104 (2000) 8124.
[19] K. Kleykamp, Z. Phys. Chem. N.F. 71 (1970) 142.
[20] G. Artioli, et al., in preparation.
[21] A.K. Datye, J. Bravo, T.R. Nelson, P. Atanasova, M. Lyubovsky, L. Pfefferle, Appl. Catal. 198 (2000) 179.
[22] R. Burch, F.J. Urbano, Appl. Catal. A 124 (1995) 121.
[23] Unpublished results from our labs.
[24] J.N. Carstens, S.C. Su, A. Bell, J. Catal. 176 (1998) 136.
[25] G. Groppi, W. Ibashi, M. Valentini, P. Forzatti, Chem. Eng. Sci. 56 (2001) 831.
[26] K. Otto, L.P. Haack, J.E. de Vries, Appl. Catal. B 1 (1992) 1.
[27] M. Lyubovsky, L. Pfefferle, Appl. Catal. A 173 (1998) 107.
[28] F. Ribeiro, M. Chow, R.A. Dalla Betta, J. Catal. 146 (1994) 537.
[29] Y.Y. Yao, Ind. Eng. Chem. Prod. Res. Dev. 19 (1980) 293.
[30] R.F. Hicks, M.L. Young, R.G. Lee, J. Catal. 122 (1990) 295.
[31] S.H. Oh, P.J. Mitchell, R.M. Siewert, J. Catal. 132 (1991) 287.
[32] P. Briot, M. Primet, Appl. Catal. 68 (1991) 301.
[33] T.R. Baldwin, R. Burch, Appl. Catal. 66 (1990) 337.
[34] C.A. Muller, M. Macieijewski, R.A. Koeppel, A. Baiker, Catal. Today 47 (1999) 245.
[35] K. Fujimoto, F. Ribeiro, M. Avalos-Borja, E. Iglesia, J. Catal. 179 (1998) 431.
[36] E. Garbowski, M. Primet, Appl. Catal. A 125 (1995) 185.
[37] T.R. Baldwin, R. Burch, Catal. Lett. 6 (1990) 131.
[38] R.S. Monteiro, D. Zemlyanov, J.M. Storey, F.H. Ribeiro, J. Catal. 199 (2001) 37.
[39] R.S. Monteiro, D. Zemlyanov, J.M. Storey, F.H. Ribeiro, J. Catal. 199 (2001) 291.
[40] J. Au-Yeung, A.T. Bell, E. Iglesia, J. Catal. 185 (1999) 213.
[41] J.C. van Giezen, F.R. van den Berg, J.L. Kleinen, A.J. van Dillen, J.W. Geus, Catal. Today 47 (1999) 287.

[42] T.R. Badwin, R. Burch, Appl. Catal. A 66 (1990) 337.
[43] R.A. Dalla Betta, J.C. Schlatter, D.Y. Kee, D.G. Loffler, T. Shoji, Catal. Today 26 (1995) 329.
[44] W. Ibashi, G. Groppi, P. Forzatti, 5IWCC, 5IWCC, Seoul, 2002.
[45] M. Machida, K. Eguchi, H. Arai, Chem. Lett. (1987) 767.
[46] G. Groppi, M. Bellotto, C. Cristiani, P. Forzatti, P.L. Villa, Appl. Catal. A 104 (1994) 101.
[47] M. Machida, K. Eguchi, H. Arai, J. Catal. 103 (1987) 85; M. Machida, K. Eguchi, H. Arai, J. Catal. 120 (1989) 377.
[48] M. Bellotto, G. Artioli, C. Cristiani, P. Forzatti, G. Groppi, J. Catal. 179 (1998) 597.
[49] M. Machida, K. Eguchi, H. Arai, J. Catal. 123 (1990) 477.
[50] G. Groppi, C. Cristiani, P. Forzatti, Catalysis 13 (1997) 85.
[51] G. Groppi, C. Cristiani, P. Forzatti, Appl. Catal. B 35 (2001) 137.
[52] A.J. Zarur, J.Y. Ying, Nature 403 (2000) 65.
[53] A.J. Zarur, H.H. Hwu, J.Y. Ying, Langmuir 16 (2000) 3042.
[54] M.M. Wolf, H. Zhu, W.H. Green, G.S. Jackson, Appl. Catal. A 244 (2003) 323.
[55] M. Wolf, personal communication.
[56] R.J. Kee, F.M. Rupley, E. Meeks, J.A. Miller, CHEMKIN-III, 1996.
[57] R.A. Dalla Betta, J.C. Schlatter, D.K. Yee, D.G. Loffler, T. Shoji, Catal. Today 26 (1995) 329.
[58] Y. Tsujikawa, S. Fujii, H. Sadamori, S. Ito, S. Katsura, ASME Paper 5-GT-351, 1995.
[59] R.A. Dalla Betta, D.G. Loffler, ACS Symp. Ser. Heterogeneous Hydrocarbon Oxidation 628 (1996) 36.
[60] D. Leung, R.E. Hayes, S.T. Kolackzowski, Can. J. Chem. Eng. 74 (1996) 94.
[61] G. Groppi, E. Tronconi, P. Forzatti, Catal. Rev. Sci. Eng. 41 (1999) 227.
[62] L.L. Raja, R.J. Kee, O. Deutschmann, J. Warnatz, L.D. Schmidt, Catal. Today 59 (2000) 47.
[63] S. Kajita, R. Dalla Betta, 5IWCC, Seoul, 2002.
[64] M. Lyubovski, R. La Pierre, L. Smith, M. Castaldi, B. Netwick, W.C. Pfefferle, 5IWCC, Seoul, 2002.
[65] D.L. Trimm, Z.I. Onsan, Catal. Rev. 43 (2001) 31.
[66] R. Burch, P.K. Loader, Appl. Catal. A 122 (1995) 169.
[67] A. Beretta, P. Forzatti, 2002, submitted for publication.
[68] J.R. Rostrup-Nilesen, J. Catal. 31 (1973) 173.
[69] J. Rostrup-Nielsen, J.H. Bak Hansen, J. Catal. 144 (1993) 38.
[70] S.C. Tsang, J.B. Claridge, M.L.H. Green, Catal. Today 23 (1995) 3.
[71] D.A. Hickman, L.D. Schmidt, Science 259 (1993) 343.
[72] P.M. Witt, L.D. Schmidt, J. Catal. 163 (1996) 465.
[73] A.S. Bodke, S.S. Bharadway, L.D. Schmidt, J. Catal. 194 (1998) 138.
[74] L. Basini, K. Aasberg-Petersen, A. Guarinoni, M. Ostberg, Catal. Today 64 (2001) 9.
[75] J.K. Hochmuth, Appl. Catal. B 1 (1992) 89.